Chimica Techno Acta
published by Ural Federal University
eISSN2411-1414; chimicatechnoacta.ru

ARTICLE
2022, vol. 9(4), No. 20229419
DOI: 10.15826/chimtech.2022.9.4.19

Substituted benzocoumarin derivatives: synthesis, characterization, biological activities and molecular docking with ADME studies

Megha G.V. [a], Yadav D. Bodke [a*], Shanavaz H. [b], Muthipeedika Nibin Joy [c]

a: Department of PG Studies and Research in Chemistry, Jnana Sahyadri, Kuvempu University, Shankaraghatta 577451, Karnataka, India
b: Department of Chemistry, Faculty of engineering and technology, Jain University, Kankapura 562112, Karnataka, India
c: Innovation Center for Chemical and Pharmaceutical Technologies, Institute of Chemical Technology, Ural Federal University, Yekaterinburg 620002, Russia
* Corresponding author: ydbodke@gmail.com

This paper belongs to a Regular Issue.

Abstract

Herein, we report an efficient and convenient method for the synthesis of 4-(substitutedphenyl)-1,2-dihydro-2-oxo-6-(2-oxo-2H-benzo[g]chromen-3-yl)pyridine-3-carbonitrile derivatives using ammonium acetate as a catalyst. The structures of the synthesized compounds were confirmed using FT-IR, ^{1}H, ^{13}C-NMR and LC-MS spectroscopic techniques. The synthesized compounds were evaluated for antibacterial activity against bacterial strains by disc diffusion method at different concentrations. Further, all the targeted compounds were screened for anti-oxidant and anti-cancer studies by DPPH and MTT assay methods respectively at different concentrations. Compound **4b** displayed good antioxidant and anticancer (against MCF-7 cell line) activity. The binding capability for the synthesized compounds (**4a–j**) was analyzed by molecular docking studies using human peroxiredoxin 5 (PDB ID: 1HD2) and P38 MAP kinase (PDB ID: 1OUK) protein. The physicochemical properties were analyzed using absorption, distribution, metabolism and excretion (ADME) studies.

Keywords

benzo-coumarin
anti-bacterial
anti-cancer
anti-oxidant
molecular docking

Received:11.10.22
Revised: 08.11.22
Accepted: 09.11.22
Available online: 16.11.22

1. Introduction

Coumarin is a well-known naturally occurring organic compound, and it has been utilised in various fields such as pharmaceuticals. Around the world, research is being conducted on this compound due to its properties [1]. Coumarins are naturally occurring active constituents of various plants such as *Dipteryxodorata, Anthoxanthumodoratum, Galiumodoratum*, etc, [2]. These are found in higher plants like *Rutaceaeand Umbelliferae* and essential oils of cinnamon bark, cassia leaf, and lavender oil [3]. *Coumarin* is an aromatic compound that has a bicyclic structure with lactone carbonyl groups. The presence of an electronegative atom is effective for hydrogen bond formation and for solubility, to some extent, and the aromatic ring is responsible for having hydrophobicity. These phenomena are the cause of better interaction of the molecule with a receptor site. The substitution of coumarins activates their bioactivity. For thousands of years, natural products have been utilized in the traditional medicines, in addition to their use as a promising source of components for discovery and development of new therapies [4]. Numerous types of coumarins have been synthesized with different types of substitutions or pharmacophore in their basic nuclei, which are significant in showing effective and diverse classes of biological activity [5]. Based on the substitution pattern, coumarins show anticancer [6], anti-HIV [7], anticoagulant [8], antimicrobial [9], antioxidant [10], antihypertensive [11], antihyperglycemic [12], antituberculosis [13], and anti-inflammatory [14] activities.

Cancer is a chronic disease that is associated with multiple syndromes and, hence, its treatment requires close attention. World Health Organization (WHO) reported in 2013 that a not-contagious illness such as cancer is responsible for 60% deaths worldwide. Among them, 80% of deaths (28 million) occur in low and middle- income countries like India [15]. A number of anticancer agents are currently used in clinical practice for treatment of various kinds of cancers. Coumarin and its derivatives possess anticancer activity against different types of cancers such as prostate, renal, breast, laryngeal, lung, colon, CNS,

leukemia, malignant melanoma [16–18]. Breast cancer is the most frequent in females, and it is one of the leading causes of cancer death for women. Breast cancer can also occur in men, but it is far less common. Yet new treatment methods provide more reason for optimism than ever before [19]. Coumarin derivatives readily interact with a variety of enzymes and receptors in breast cancer cells. Moreover, the coumarin-based irosustat drug is known to interact with sulfatase enzyme, indicating that coumarin derivatives are potential materials for anti-breast cancer agents [20]. In the last 30 years, doctors have made great strides in early diagnosis and treatment of the disease and in reducing breast cancer deaths. There are many chemotherapy agents available for the treatment of breast cancer. Still, the current therapeutic options have not fulfilled the desired outcomes for breast cancer therapy [21]; thus, there is an urgent need to develop novel synthetic coumarin derivatives with anti-breast cancer potential.

2. Experimental

2.1. Materials and Method

The reagents, solvents and chemicals were purchased from Sigma-Aldrich and were used without further purification. Alumina TLC plates were used to check the progress of the reaction. The spots were identified in a 360 nm UV chamber. The melting points were determined by the electro-thermal apparatus using open capillary tubes and are uncorrected. FTIR spectra were recorded on a Bruker spectrophotometer using KBr pellets in the region of 400–4000 cm^{-1}. ^{1}H-NMR and ^{13}C-NMR (400 MHz and 100 MHz) spectra were recorded using a Jeol instruments and estimated with the Delta software in DMSO-d_6 solvent system; chemical shifts (δ) were recorded in ppm relative to tetramethyl silane as a standard reference. The molecular weight of synthesized compounds was confirmed by a LC-MS 2010, SHIMADZU, mass analyzer. Elemental analysis was performed by using the unique method. The anti-bacterial activity was carried out against two Gram-negative and Gram-positive bacterial strains using the agar diffusion method and anti-oxidant by DPPH scavenging activity at different concentrations. The anti-cancer activity was tested against MCF-7 cell line by the MTT method at different concentrations and compared with a standard drug.

2.2. General procedure for the synthesis of 4-(substitutedphenyl)-1,2-dihydro-2-oxo-6-(2-oxo-2H-benzo[g]chromen-3-yl)pyridine-3-carbonitrile derivatives 4(a–j)

In a 100 mL round bottom flask, an equimolar mixture of 3-acetyl benzocoumarin (**1**, 1 mmol), substituted aromatic aldehydes (**2**, 1 mmol) and ethylcyanoacetate (**3**, 1 mmol), was taken in 20 mL of ethanol, and ammonium acetate (8 mmol) was added as catalyst. The reaction mixture was refluxed for about 8 h, and after the completion of the reaction (monitored by TLC using ethyl acetate: petroleum ether in the 1:4 ratio) the solid compound separated was filtered, washed thoroughly and recrystallized from absolute ethanol to get pure compounds. The analytical are given in Table 1.

Table 1 Analysis and specification of synthesized compounds (**4a–j**).

Entry	R^1	R^2	R^3	Compound	Yield, %
4a	NO_2	H	H	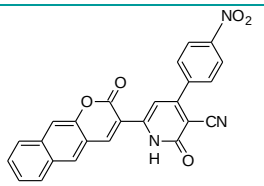	70
4b	Br	H	H	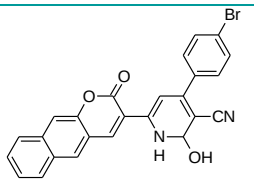	74
4c	Cl	H	H	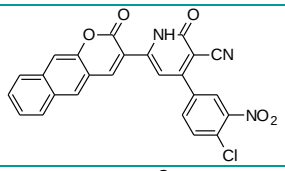	72
4d	CN	H	H	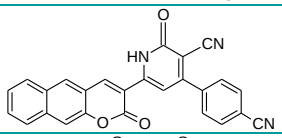	76
4e	OH	OCH_3	H	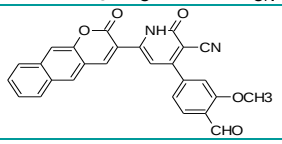	71
4f	H	NO_2	H	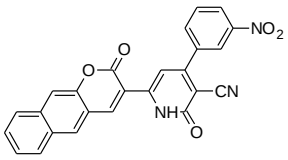	74
4g	Cl	H	H	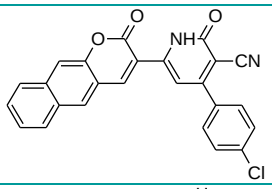	78
4h	Indole	H	H	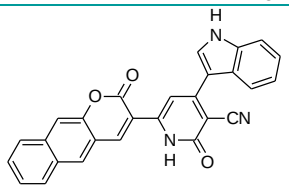	81
4i	H	H	Br	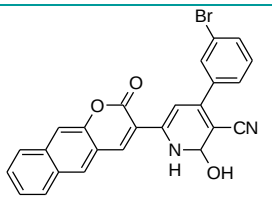	76
4j	OCH_3	H	H	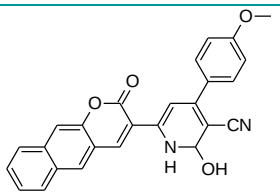	82

2.2.1. 4-(4-Nitrophenyl)-1,2-dihydro-2-oxo-6-(2-oxo-2H-benzo[g]chromen-3-yl)pyridine-3-carbonitrile (4a)

Orange solid, yield-70%, M.P. > 300 °C; FTIR (KBr, υ cm^{-1}): 3459 (NH), 2204 (C≡N), 1733 (C=O) ,1610 (C=C), 1307 (C–C); ^{1}H-NMR (400 MHz, DMSO-d_6, δ ppm): 7.26 (*s*, 1H, Ar–CH), 7.62–7.58 (*t*, 2H, Ar–H), 7.82 (*s*, 1H, Ar–H), 8.04–8.03 (*d*, *J* = 6.8 Hz, 2H, Ar–H), 8.35–8.32 (*d*, *J* = 8 Hz, 3H, Ar–H) 8.56–8.53 (*d*, *J* = 12 Hz,1H, Ar–H), 9.50 (*s*, 1H, NH); ^{13}C NMR (100 MHz, DMSO–d_6, δ ppm): 94.22 (C–C), 116 (C–C≡N), 119.14, 120.17, 123.59, 126.59, 129.75, 129.08, 129.511, 130.46, 130.46, 133.11, 134.52, 139.006, 140.59, (C=C), 170 (C=O), 159 (C=o); LCMS: *m/z* 436.04 $[M+H]^+$. Anal. Calcd. for $C_{25}H_{13}N_3O_5$: C 71.25%; H 3.59%; N 9.97%. Found: C 68.25%; H 2.58%; N 9.87%.

2.2.2. 4-(4-Bromophenyl)-1,2-dihydro-2-oxo-6-(2-oxo-2H-benzo[g]chromen-3-yl)pyridine-3-carbonitrile (4b)

Pale orange solid, yield-74%, M.P. > 300 °C; FTIR (KBr, υ cm^{-1}): 3426 (NH), 2222.59 (C≡N), 1733 (C=O), 1351 (C–C), 605(C–Br). ^{1}H-NMR (400 MHz, DMSO-d_6, δ ppm): 7.26 (*s*, 1H, Ar–CH), 7.61–7.58 (*dd*, *J* = 12 Hz, 2H, Ar–H), 7.63–7.63 (*d*, 1H, Ar–H), 7.74–7.72 (*d*, *J* = 8 Hz, 1H, Ar–H), 7.83–7.81 (*d*, *J* = 8 Hz, 1H, Ar–H) 8.06–8.02 (*t*, 2H, Ar–H), 8.23–8.21 (*d*, *J* = 8 Hz 1H, Ar–H), 8.34–8.31 (*d*, *J* = 12Hz, 2H, Ar–H), 8.55–8.53 (*d*, *J* = 8 Hz, 1H, Ar–H), 9.499 (*s*, 1H, NH) ;^{13}C NMR (100 MHz, DMSO-d_6, δ ppm): 116.92 (C–C≡N), 122.88, 122.90, 123.13, 126.77, 128.63, 129.08, 129.38, 129.51, 129.55, 129.68, 130.53, 130.81, 132.58 148.58 (C=C), 152.95 (C=O), 153.54 (C=O); LCMS: *m/z* 470.98 $[M+H]^+$. Anal. Calcd. for $C_{25}H_{13}BrN_2O_3$: C 66.54%; H 3.65%; N 5.97%. Found: C 64.25%; H 3.58%; N 4.87%.

2.2.3. 4-(4-Chloro-3-nitrophenyl)-1,2-dihydro-2-oxo-6-(2-oxo-2H-benzo[g]chromen-3-yl)pyridine-3-carbonitrile (4c)

Yellow solid, yield-72%, M.P. > 300 °C; FTIR (KBr, υ cm^{-1}): 3414 (NH), 2206(C≡N), 1637 (C=O), 617(C–Cl). ^{1}H-NMR (400 MHz, DMSO-d_6, δ ppm): 7.22 (*s*, 1H, Ar–CH), 7.67–7.62 (*dd*, 2H, Ar–H), 7.89–7.79 (*d*, *J* = 8 Hz, 2H, Ar–H), 7.94–7.93 (*d*, *J* = 4.4Hz, 1H, Ar–H), 8.10–8.08 (*d*, *J* = 8 Hz, 1H, Ar–H) 8.27–8.25(*d*, *J* = 8 Hz, 2H, Ar–H), 8.56 (*s*, 1H, Ar–H), 8.59 (*s*, 1H, Ar–CH), 9.510 (*s*, 1H, NH); ^{13}C-NMR (100 MHz, DMSO-d_6, δ ppm): 107.90 (C–CH), 116.91, 122.48, 125.69, 126.99, 129.22, 129.56, 130.51, 132.67, 133.92, 137.69, 140.54 148.19 (C=C), 154.69, 154.19, (C=O); LCMS: *m/z* 470.00 $[M+H]^+$. Anal. Calcd. for $C_{25}H_{12}ClN_3O_5$: C 63.91%; H 2.57%; N 8.94%. Found: C 62.90%; H 1.58%; N 9.87%.

2.2.4. 4-(4-Cyanophenyl)-1,2-dihydro-2-oxo-6-(2-oxo-2H-benzo[g]chromen-3-yl)pyridine-3-carbonitrile (4d)

Orange red solid, yield-76%, M.P. > 300 °C; FTIR (KBr, υ cm^{-1}): 3416 (NH), 2029 (C≡N), 1717 (C=O), 1570 (C=C), 1307(C–C);^{1}H-NMR (400 MHz, DMSO-d_6, δ ppm): 7.18 (*s*, 1H, Ar–CH), 7.59–7.57 (*d*, *J* = 8 Hz, 1H, Ar–H), 7.63–7.61 (*d*, *J* = 8 Hz, 2H, Ar–H) 7.74–7.70 (*d*, *J* = 8 Hz, 3H, Ar–H), 7.96–7.94 (*d*, *J* = 8 Hz, 2H, Ar–H) 8.05–8.03 (*d*, *J* = 8 Hz, 1H, Ar–H) , 8.21–8.19 (*d*, *J* = 8 Hz, 1H, Ar–H), 8.53–8.51 (*d*, *J* = 8 Hz, 1H, Ar–H), 9.49 (*s*, 1H, NH) ; ^{13}C NMR (100 MHz, DMSO-d_6, δ ppm): 82.81 (C–C), 95.03 (C–C), 116.88 (C≡N), 120.27, 127.85, 123.85, 123.12, 123.83, 126.72, 126.77, 128.64, 129.07, 129.51, 129.68, 130.47, 134.11, 136.44, 148.86 (C=C), 153.51 (C–NH), 169 (C=O); LCMS: *m/z* 416.07 $[M+H]^+$. Anal. Calcd. for $C_{26}H_{13}N_3O_3$: C 75.18%; H 3.15%; N 10.12%. Found: C 71.90%; H 2.14%; N 9.87%.

2.2.5. 4-(Hydroxy-3-Methylphenyl)-1,2-dihydro-4-2-oxo-6-(2-oxo-2H-benzo[g]chromen-3-yl)pyridine-3-carbonitrile (4e)

Pale yellow solid, yield-71%, M.P. > 300 °C; FTIR (KBr, υ cm^{-1}); 3414 (NH), 2924 (OCH_3), 2202 (C≡N), 1635 (C=O), 1386(C=C); ^{1}H-NMR (400 MHz, DMSO-d_6, δ ppm): 3.92 (*s*, 3H, OCH_3), 6.92 (*s*, 1H, Ar–CH), 7.40–7.38 (*d*, *J* = 8 Hz, 2H, Ar–H), 7.66–7.65 (*d*, *J* = 4 Hz, 2H, Ar–H), 7.82–7.80 (*d*, *J* = 8 Hz, 2H, Ar–H) 7.89–7.83 (*s*, 1H, Ar–H), 8.10–8.08 (*d*, *J* = 8 Hz, 2H, Ar–H) 8.35–8.28 (*s*, 1H, Ar–H), 9.503 (*s*, 1H, NH), 9.753 (*s*, 1H, OH) ;^{13}C-NMR (100 MHz, DMSO-d_6, δ ppm): 63.33 (OCH_3), 110.54, 113.46 (C–C), 116.86 (C≡N), 117.5, 118.45, 123.30, 126.71, 129.52, 130.47, 131.04, 135.24, 135.38, 143.79, 148.06, 148.33 (C=C), 167.14 (C=O); LCMS: *m/z* 449.13 $[M+H]^+$. Anal. Calcd. for $C_{26}H_{13}N_3O_3$: C 72.32%; H 3.60%; N 6.25%. Found: C, 71.90%; H 2.14%; N 5.87%.

2.2.6. 3-(Nitrophenyl)-1,2-dihydro-4-2-oxo-6-(2-oxo-2H-benzo[g]chromen-3-yl)pyridine-3-carbonitrile(4f)

Pale orange solid, yield-74%, M.P. > 300 °C; FTIR (KBr, υ cm^{-1}): 3415 (NH), 2202 (C≡N), 1732 (C=O), 1347 (C–C), 1621 (C=C); ^{1}H-NMR (400 MHz, DMSO-d_6, δ ppm): 7.45 (*s*, 1H, Ar–H), 7.67–7.65 (*dd*, *J* = 8 Hz, 3H, Ar–H), 7.70–7.68 (*d*, *J* = 8 Hz, 2H, Ar–H), 7.80 (*s*, 1H, Ar–H), 7.83–7.81 (*d*, *J* = 8 Hz, 1H, Ar–H) 8.12–8.10 (*d*, *J* = 8 Hz, 1H, Ar–H), 8.35–8.32 (*d*, *J* = 8 Hz, 1H, Ar–H), 8.70–8.68 (*d*, *J* = 8 Hz, 2H, Ar–H), 9.21 (*s*, 1H, Ar–H), 9.47 (*s*, 1H, NH) ; ^{13}C-NMR (100 MHz, DMSO-d_6, δ ppm): 95.72 (C–C), 107.50 (C–C), 113.56 (C=C), 116.87 (C–C≡N), 122.87, 123.87, 123.12, 12.49, 126.80, 129.12, 129.52, 130.46, 130.94, 134.87, 135.21, 139.56, 139.56, 139.83, 148.31 (C=C), 159.53(C=O); LCMS: *m/z* 436.04 $[M+H]^+$. Anal. Calcd. For $C_{26}H_{13}N_3O_3$: C 68.97%; H 3.01%; N 9.65%. Found: C 65.90%; H 2.14%; N 5.87%.

2.3. Pharmacological activities

2.3.1. Antibacterial activity

The four bacterial strains *Bacillus subtilis, Staphylococcus aureus* (gram-positive bacteria) and *Escherichia coli, Pseudomonas aeruginosa* (Gram-negative bacteria) were used to investigate the antibacterial activity of the synthesized compounds (**4a–j**) by the disk diffusion method [22]. Briefly, all the compounds were dissolved in DMSO in two different concentrations (25 and 50 mg/mL), and to this test solution, the previously cultured Mueller Hinton Agar Sabouraud's dextrose agar medium was added and autoclaved at ±37 °C for about 24 h. Streptomycin was used as

a standard drug and 10% DMSO used as a negative control. The antimicrobial assay of the title compounds was measured by the formed zone of inhibition against pathogenic strains. The test was performed in triplicate and the average was taken as a final reading. The minimum inhibitory concentration (MIC) was determined by the serial broth-dilution method [23].

2.3.2. Antioxidant activity

The synthesized compounds (**4a–j**) were screened for DPPH scavenging activity [24], and DPPH methods were carried out according to the reported procedure [25, 26]. The compounds at different concentrations (5 μg/mL, 10 μg/mL, 20 μg/mL, 40 μg/mL, 80 μg/mL) were used for the analysis. Ascorbic acid was choosing for comparison as a standard drug and Radical scavenging activities were calculated using the formula [27]:

$$\% \text{ inhibition} = [(A_{control} - A_{test})/A_{control}]\cdot 100, \quad (1)$$

where $A_{control}$ is the absorbance of the control reaction and A_{test} is the absorbance of the synthesized compound. IC_{50} value was calculated using the formula: $IC_{50} = [(C/\Sigma I)\cdot 50]$, where ΣC is the sum of synthesized compound concentrations used to test and ΣI is the sum of % of inhibition at different concentration. Each value is expressed as a mean ±SD of three replicates.

2.3.3. Cytotoxicity

The *in vitro* cytotoxicity was assessed by MTT assay by following the procedure of Kumbar et al. [28], against the MCF-7 (Breast cancer) cell line. The cells were seeded in a 96-well flat-bottom microplate and maintained at 37 °C in 95% humidity and 5% CO_2 overnight. Different concentrations (200, 100, 50, 25, 12.5 and 6.25 μg/mL) of the samples were treated. The cells were incubated for another 48 h, and the wells were washed twice with PBS. 20 μL of the MTT staining solution was added to each well, and the plate was incubated at 37 °C. After 4 h, 100 μL of DMSO was added to each well to dissolve the formazan crystals, and absorbance was recorded at 570 nm using a microplate reader. The percentage of cell survival was calculated by using the following formula [29, 30].

$$\% \text{ of cell survial} = \frac{\text{Mean OD of Test compound}}{\text{Mean OD of Negative control}} \cdot 100 \quad (2)$$

2.3.4. *In silico* Molecular docking study

The molecular interactions of the synthesized compounds at the binding pocket of human peroxiredoxin 5 protein and P38 MAP kinase proteins were studied using automated docking by employing the Autodock Vina program [31]. The co-crystallized structure of human peroxiredoxin 5 protein (PDB ID: 1HD2) and P38 MAP kinase (PDB ID: 1OUK) were retrieved from the protein databank, and their substrate binding sites were identified using the pdb sum server [32]. A grid box of dimensions 20x20x20 Å with *X*, *Y* and *Z* coordinates at 7.654, 40.848 and 34.184 for human peroxiredoxin 5 and 20x20x20 Å with *X*, *Y* and *Z* coordinates at 44.438, 32.882 and 32.692 for P38 MAP kinase were created, respectively. The grid box was set around the residues forming the active pocket. The binding interactions were visualized using Biovia Discovery Studio Visualizer V.20.1.

2.3.5. *In silico* oral bioavailability assessment and ADME

Various physicochemical features and pharmacokinetic descriptors were calculated through the online web tool Swiss ADME [33]. The oral bioavailability of the synthesized compounds (**4a–j**) was predicted using the Lipinski rule-of-five (RO5) filter [34] to derive the candidate drug pharmacokinetic (PK). The structural properties used in the RO_5 filter are derived using Osiris Data warrior V.4.4.3 software [35]. The bioavailability scores were predicted using the molinspiration server [36].

3. Results and Discussions

3.1. Chemistry

In the present study, we developed a simple, convenient and environmentally safe method for the synthesis of some new 4-(substitutedphenyl)-1,2-dihydro-2-oxo-6-(2-oxo-2H-benzo[g]chromen-3-yl)pyridine-3-carbonitrile derivatives (**4a–j**) via the one-pot reaction of 3-acetyl benzocoumarin (**1**), substituted aromatic aldehydes (**2**) and ethyl cyanoacetate (**3**) in ethanol using ammonium acetate as a catalyst (Scheme 1).

3.2. Biological activity

3.2.1. Antibacterial activity

The *in vitro* antibacterial activity of the synthesized compounds was screened against four pathogenic strains and the results are tabulated in Table 2. The result revealed that all the test compounds exerted a varied degree of antibacterial activity against the tested strains. Further, to quantify the lowest concentration at which the growth of the organism was prevented, we determined the minimum inhibitory concentration (MIC). The results are given in Table 3. Compounds **4a, 4c, 4h** and **4i** exhibited equipotent activity against *E. coli*, *Pseudomonas aeruginosa* and *S. Aureus* with MIC 2.1–2.3 mg/ml.

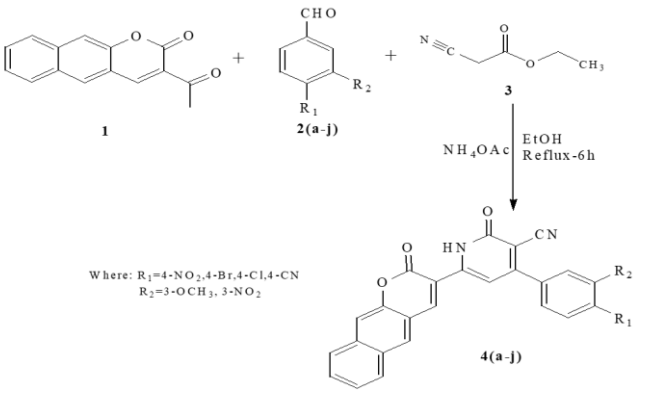

Scheme 1 Synthesis of 4-(substitutedphenyl)-1,2-dihydro-2-oxo-6-(2-oxo-2H-benzo[g]chromen-3-yl) pyridine-3-carbonitrile derivatives (**4a–j**).

From the structure activity relationship studies, it was observed that compounds **4e** and **4j**, having methoxy groups on the aromatic ring, showed excellent activity among the series when compared to the standard drug. Compounds **4a, 4c, 4f** and **4g,** having $-NO_2$ and –Cl groups, respectively, displayed promising activity against *B.* subtilis. The rest of the synthesized compounds showed moderate activity against selected bacterial strains.

3.2.2. Antioxidant activity

The synthesized compounds (**4a–j**) were screened for their free radical scavenging activity by the DPPH method as shown in Figure 1. All the compounds showed varied free radial scavenging capacity in assessment with the standard Ascorbic acid. Among all the compounds, compound **4b** exhibited most effective antioxidant efficacy with IC_{50} value 34.66±2.43 µg/mL as compared to the reference standard drug (IC_{50} 8.88±1.19 µg/mL). Compounds **4a**, **4c**, **4f** and **4j** with IC_{50} in the range of 41.54–44.11 µg/mL showed promising antioxidant activity, and the rest of the compounds showed moderate scavenging activity by the DPPH method. Therefore, the synthesized compounds exhibited more effective antioxidant efficacy due to the presence of the electron donating group (OH) at para position of the phenyl ring [37]. The results are shown in Table 4.

3.2.3. Cytotoxicity study

The *in vitro* cytotoxicity of the synthesized compounds (**4a–f**) was evaluated against the MCF-7 (Breast cancer) cell line and shown in Figure 2. A graph detailing the concentration versus survival fraction of the compounds was plotted in Figures 3 and 4, and the results were expressed as the half-maximal inhibitory concentrations (IC_{50}) (Table 5) with Doxorubicin as a standard drug. The cytotoxicity results suggested that the test compounds have a very good selectivity against the MCF-7 cell line. The cytotoxicity data revealed that compound **4d** possessed significant IC_{50} values of 22.60±0.30 µg/mL as compare to the standard drug. The remaining compounds displayed considerable selectivity with IC_{50} values in the range of 37.10±0.36 to 193.97±3.71 µg/mL.

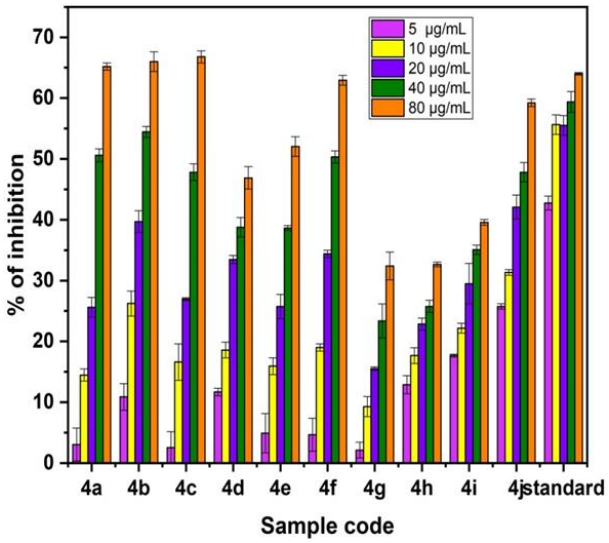

Figure 1 Antioxidant activity of synthesized compounds (c).

Table 2 Bacterial studies of synthesized compounds (**4a–j**).

Compound	*B. subtilis*		*S. aureus*		*E. coli*		*P. aeruginosa*	
	25 mg/ml	50 mg/ml	25 mg/ml	50 mg/ml	25 mg/ml	50 mg/ml	25 mg/ml	50 mg/ml
4a	1.5±0.3	1.9±0.5	1.3±0.12	1.5±0.24	1.2±0.6	1.7±0.8	1.2±0.15	1.6±0.24
4b	2.0±0.12	2.4±0.12	1.8±0.12	2.0±0.21	1.6±0.2	1.8±0.5	2.1±0.25	2.4±0.21
4c	2.0±0.1	2.1±0.4	1.7±0.2	2.1±0.21	1.5±0.22	1.8±0.23	1.8±0.12	1.9±0.26
4d	1.4±0.24	1.7±0.29	1.9±0.23	1.8±0.22	1.8±0.1	2.2±0.30	1.8±0.15	2.1±0.28
4e	1.0±0.21	1.7±0.24	1.0±0.21	2.4±0.25	1.0±0.15	1.4±0.21	1.7±0.2	1.8±0.23
4f	2.0±0.12	2.3±0.21	2.0±0.12	2.3±0.21	1.8±0.23	2.1±0.24	1.6±0.18	2.1±0.23
4g	2.5±0.3	1.9±0.26	2.4±0.25	1.7±0.8	1.6±0.18	2.4±0.12	1.6±0.18	1.7±0.8
4h	1.8±0.12	2.4±0.12	2.1±0.24	1.9±0.26	1.7±0.24	2.2±0.30	1.5±0.22	2.4±0.12
4i	1.5±0.3	1.7±0.2	1.8±0.15	2.2±0.30	1.5±0.22	1.7±0.24	1.9±0.5	1.4±0.21
4j	2.1±0.25	2.2±0.30	1.6±0.2	1.7±0.24	1.8±0.12	2.1±0.24	1.8±0.23	1.6±0.18
Streptomycin	2.3±0.32	3.0±0.35	2.5±0.31	2.9±0.35	2.1±0.25	2.5±0.28	2.3±0.27	2.5±0.30

Table 3 MIC values of the synthesized compounds (**4a–j**).

Compound	*Bacillus subtilis*	*S. aureus*	*E. coli*	*P. aeruginosa*
4a	2.3±0.26	2.4±0.25	2.1±0.25	2.2±0.26
4b	2.4±0.32	2.1±0.29	2.3±0.25	2.2±0.25
4c	2.4±0.25	2.3±0.26	2.1±0.23	2.3±0.24
4d	2.5±0.26	2.3±0.26	2.3±0.26	2.5±0.29
4e	2.4±0.21	2.1±0.22	2.4±0.26	2.3±0.25
4f	2.5±0.21	2.4±0.23	2.1±0.25	2.3±0.26
4g	2.1±0.25	2.3±0.26	2.3±0.26	2.1±0.25
4h	2.3±0.26	2.2±0.26	2.3±0.26	2.3±0.26
4i	2.3±0.26	2.1±0.25	2.1±0.25	2.3±0.26
4j	2.5±0.26	2.4±0.23	2.3±0.26	2.3±0.26
Streptomycin	2.5±0.30	2.5±0.30	2.2±0.26	2.3±0.28

Table 4 DPPH radical scavenging activity of the synthesized compounds (**4a–j**).

Compound	DPPH radical scavenging activity % of inhibition					
	Concentration, µg/mL					
	5	10	20	40	80	IC_{50}
4a	3.054±2.71	14.47±1.00	25.63±1.61	50.59±1.05	65.20±0.60	44.11±0.50
4b	10.88±2.19	26.23±2.04	39.70±1.79	54.44±0.92	66.00±1.61	34.66±2.43
4c	2.523±2.65	16.60±2.99	26.95±0.23	47.80±1.38	66.79±1.00	44.02±0.77
4d	11.68±0.66	18.59±1.28	33.46±0.68	38.77±1.60	46.87±1.84	86.36±5.02
4e	4.913±3.22	15.93±1.37	25.75±2.00	38.64±0.04	52.05±1.61	69.33±3.37
4f	4.648±2.71	18.99±0.60	34.39±0.60	50.33±1.00	62.94±0.79	42.30±0.52
4g	2.125±1.28	9.296±1.65	15.53±0.39	23.37±2.79	32.40±2.30	194.10±12.5
4h	12.88±1.50	17.66±1.28	22.84±1.00	25.76±1.00	32.66±0.39	495.40±15.8
4i	17.66±0.22	22.17±0.82	29.48±3.32	35.06±0.79	39.57±0.46	204.37±3.85
4j	25.76±0.46	31.34±0.46	42.09±1.96	47.80±1.59	59.23±0.60	41.54±0.34
Standard	42.76±1.15	55.64±1.61	55.51±1.61	59.36±1.73	64.01±0.22	8.88±1.19

Table 5 Percentage of cell viability against MCF-7 cell line of the synthesized compounds (**4a–j**).

Compound	Mean cell Viability of MCF-7							
	NC	3.125	6.25	12.5	25	50	100	IC_{50}, µg/mL
4a	100	96.69±0.94	61.69±0.31	57.41±0.77	48.07±0.42	38.86±0.76	14.32±0.08	56.13±0.82
4b		68.15±0.53	62.48±0.85	57.13±0.94	39.05±0.84	37.52±0.14	18.87±1.95	37.10±0.36
4c		99.02±0.37	95.44±0.42	93.16±0.27	90.28±0.44	53.18±0.56	12.13±0.48	195.10±1.90
4d		99.35±0.69	95.54±0.42	91.63±0.37	90.38±0.14	88.56±0.50	33.19±0.77	22.60±0.30
4e		92.05±0.91	87.40±0.58	72.61±0.44	56.58±0.42	51.51±0.69	44.91±0.50	193.97±3.71
4f		99.58±0.28	98.14±0.32	95.56±0.65	94.09±0.66	70.01±0.14	32.82±1.08	191.03±4.94
Standard		33.80±0.67	30.57±0.42	27.53±0.37	28.56±0.43	26.15±0.17	23.69±0.53	3.16±0.10

Std – Doxorubicin, NC – Negative control
Values are Mean±SE, N = 3, *P<0.01 vs. Control.

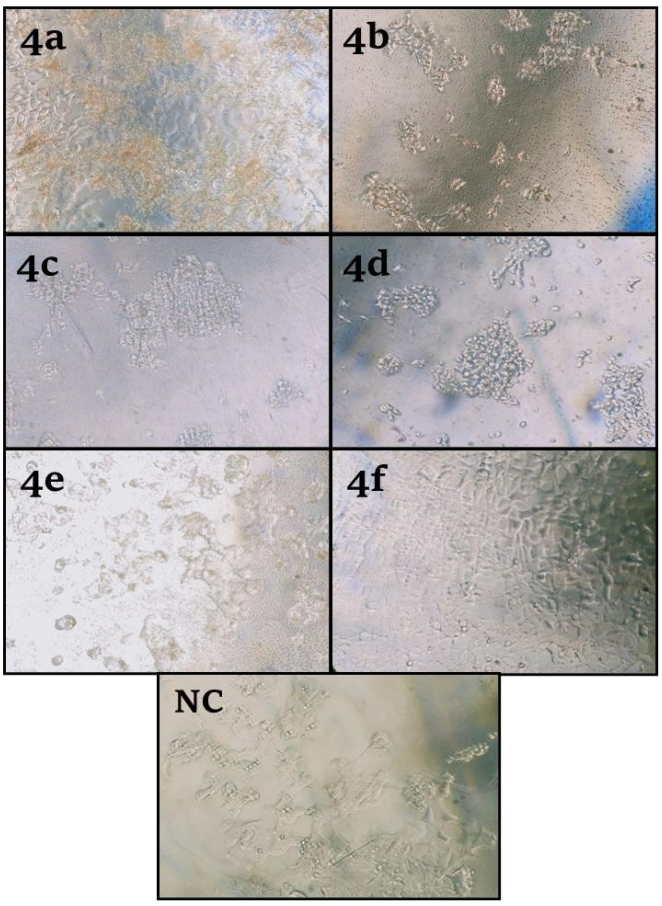

Figure 2 Images of cytotoxicity of the synthesized compounds (**4a–f**) and negative control.

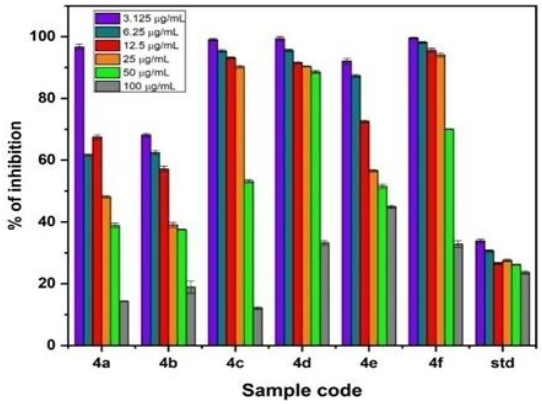

Figure 3 Graph of % of surviving cells of compounds (**4a–f**) at different concentration against MCF-7 cell line.

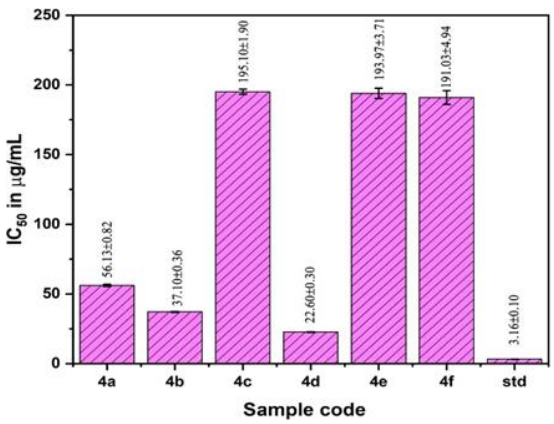

Figure 4 Graph of IC_{50} value of compounds (**4a–f**) against MCF-7 cell line.

3.2.4. *In silico* molecular docking studies

The study of intermolecular interactions between the synthesized compounds (**4a–j**) and enzymes is necessary for the development of novel therapeutic drugs [38]. Therefore, we screened the synthesized compounds for *in silico* molecular docking, which helps to predict the binding modes of the compounds with enzymes. From the results of the docking study, the synthesized compounds established good binding modes with docking receptors of Human peroxiredoxin 5 (Figures 5, 6) and P38 MAP kinase (Figures 7, 8), respectively. The docking of anti-oxidant and cytotoxicity investigations revealed that the synthesized compounds (**4a–j**) had significant docking scores in the range of –7.3 to –8.5 kcal/mol with respect to standards Ascorbic acid (–6.5 kcal/mol) and –9.8 to –11.0 kcal/mol with respect to standard Doxorubicin (–8.4 kcal/mol), respectively. The docked structures with Human peroxiredoxin 5 results suggested that compound **4h** established the lowest binding energy of –8.5 kcal/mol. The remaining compounds also established good binding modes and one or more hydrogen bonds with amino acid residues THR147, ARG127, ASN76, ARG124, GLY46, CYS47, THR44 (Table S1). The docked structures with P38 MAP kinase protein results revealed that compound **4d** demonstrated the lowest binding energy of –11.0 kcal/mol, forming one or more hydrogen bonds with three amino acid residues LYS53, VAL38, TYR35, VAL30, ALA40, LEU108. The remaining compounds also established encouraging binding energies and formed two or more hydrogen bonds with amino acid residues in their active pockets. The results are given in Table S2.

3.2.5. ADME studies

Physiochemical descriptors can be evaluated through the parameters such as molecular weight, number of heavy atoms, hydrogen bond acceptors, hydrogen bond donors, rotatable bonds, molar refractivity and topological polar surface area (TPSA). These parameters were evaluated for the synthesized compounds (**4a–j**), and the results are shown in Table 6.

The drug-likeness profiles were calculated based on Lipinski's (MW ≤ 500; HBA ≤ 10 and HBD ≤ 5) [39], Ghose (MW between 160 and 480; log *P* between –0.4 and 5.6; molar refractivity between 40 and 130, and the total number of atoms between 20 and 70), Veber (rotatable bonds ≤ 10 and TPSA ≤ 140), Egan (TPSA ≤ 131.6 Å^2) and Muegge (MW between 200 and 600; log *P* between –2 and 5; TPSA ≤ 150; number of aromatic rings ≤ 7; number of rotatable bonds ≤ 15; HBA ≤ 10 and HBD ≤ 5) [40]. All the synthesized compounds obeyed Lipinski, Ghose, Veber, Egan and Muegge rules. The rule-based score divides the compounds into four probability score classes, i.e., 11%, 17%, 55% and 85%. The acceptable probability score is 55%, which indicates that it passed the rule of five [41, 42]. The synthesized compounds (**4a–e**) showed a score of 55%, indicating that they all the five rules without any violations with good bioavailability. Further, synthetic accessibility of the compounds was assessed to quantify the complexity of the molecular structure. The results showed that the synthetic accessibility score was in the range of 3.44 to 3.67. It shows that no compound has a complex synthetic route (Table S3).

The predicted lipophilicity parameters were evaluated to study the solubility of the compounds either in aqueous or in non-aqueous medium, and they were calculated by considering the consensus logP_o/w. According to this, if the logP_o/w values are more negative, then the molecules are more soluble in nature [43]. The results showed that all the compounds have positive logP_o/w values. Hence, they are less soluble in non-aqueous medium. The values of log*S* are related to the solubility as follows if log*S* are between –10 to –6 – poorly soluble, –6 to –4 – moderately soluble, –4 to –2 – soluble, –2 to 0 – very soluble and less than 0 – highly soluble. For our synthesized compounds (**4a–j**), the log*S* value is in the range of –5.21 to –6.33; this shows that the compounds are soluble in aqueous media. The results are presented in Table S4.

The pharmacokinetic parameters such as absorption, skin permeation, distribution, metabolism and excretion were predicted. The predicted absorption and distribution parameters of the compounds are in Table S5, indicating that, all the synthesized compounds (**4a–j**) have high gastrointestinal absorption (except for **4a** and **4f**) with no blood-brain barrier crossing.

Table 6 Physicochemical properties of synthesized compounds (**4a–j**).

Code	Formula	Molecular Weight	No. Heavy atoms	HBA	HBD	Rotatable bonds	Fraction Csp^3	Molar Refractivity	TPSA
4a	$C_{25}H_{13}N_3O_5$	435.39 g/mol	33	6	1	3	0.00	125.02	132.68 Å^2
4b	$C_{26}H_{15}BrN_2O_2$	467.31 g/mol	31	2	1	2	0.04	125.65	73.72 Å^2
4c	$C_{25}H_{12}ClN_3O_5$	469.83 g/mol	34	6	1	3	0.00	130.03	132.68 Å^2
4d	$C_{26}H_{13}N_3O_3$	415.40 g/mol	32	5	1	2	0.00	120.91	110.65 Å^2
4e	$C_{27}H_{16}N_2O_5$	448.43 g/mol	34	6	1	4	0.04	128.08	113.16 Å^2
4f	$C_{25}H_{13}N_3O_5$	435.39 g/mol	33	6	1	3	0.00	125.02	132.68 Å^2
4g	$C_{25}H_{13}ClN_2O_3$	424.84 g/mol	31	4	1	2	0.00	121.21	86.86 Å^2
4h	$C_{27}H_{15}N_3O_3$	429.43 g/mol	33	4	2	2	0.00	128.05	102.65 Å^2
4i	$C_{26}H_{17}BrN_2O_2$	469.33 g/mol	31	3	2	2	0.08	128.28	73.12 Å^2
4j	$C_{26}H_{16}N_2O_4$	420.42 g/mol	32	5	1	3	0.04	122.69	96.09 Å^2

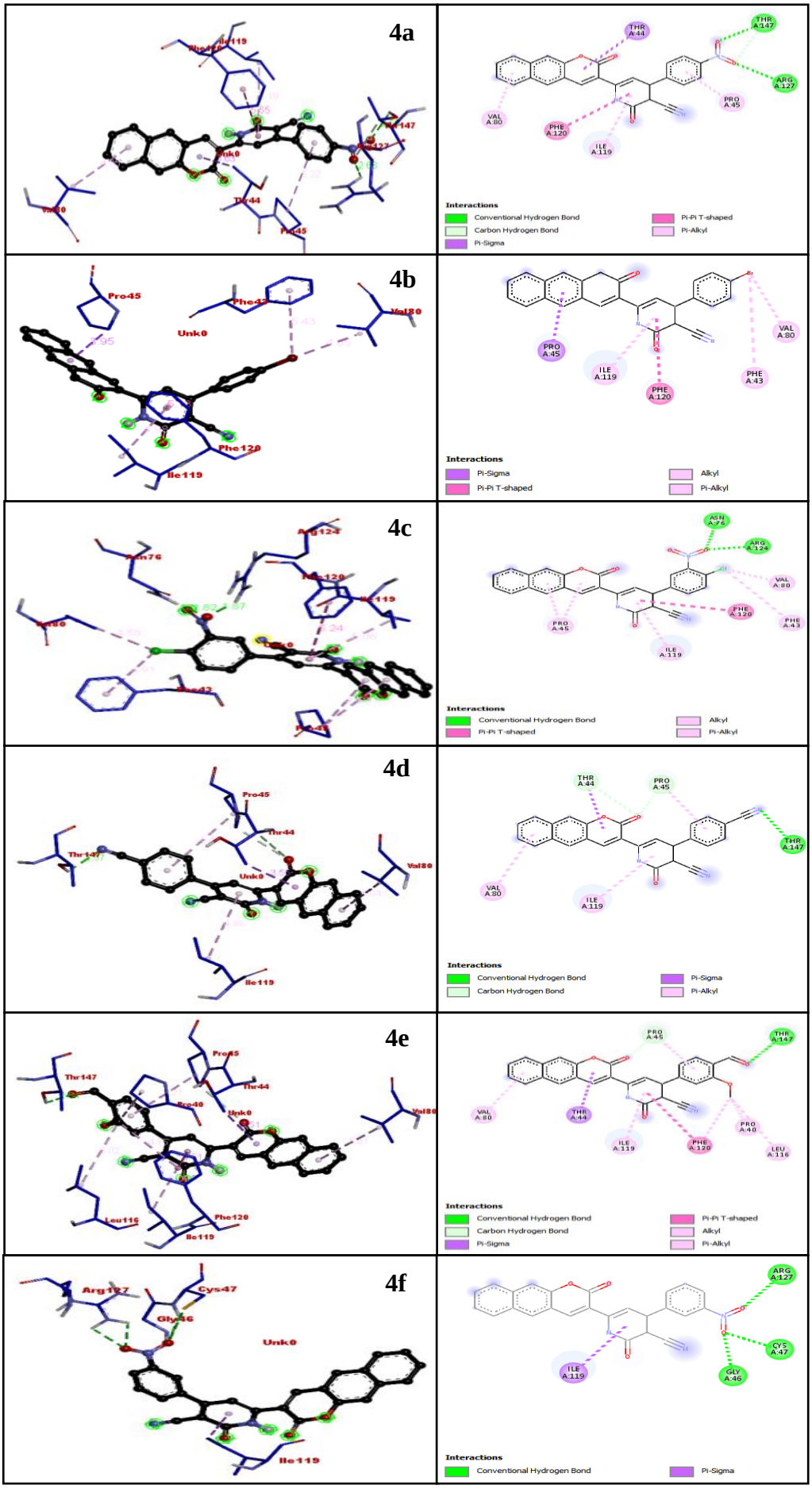

Figure 5 Three-dimensional and two-dimensional representations of molecular interactions between human peroxiredoxin 5 protein and synthesized compounds (**4a–f**).

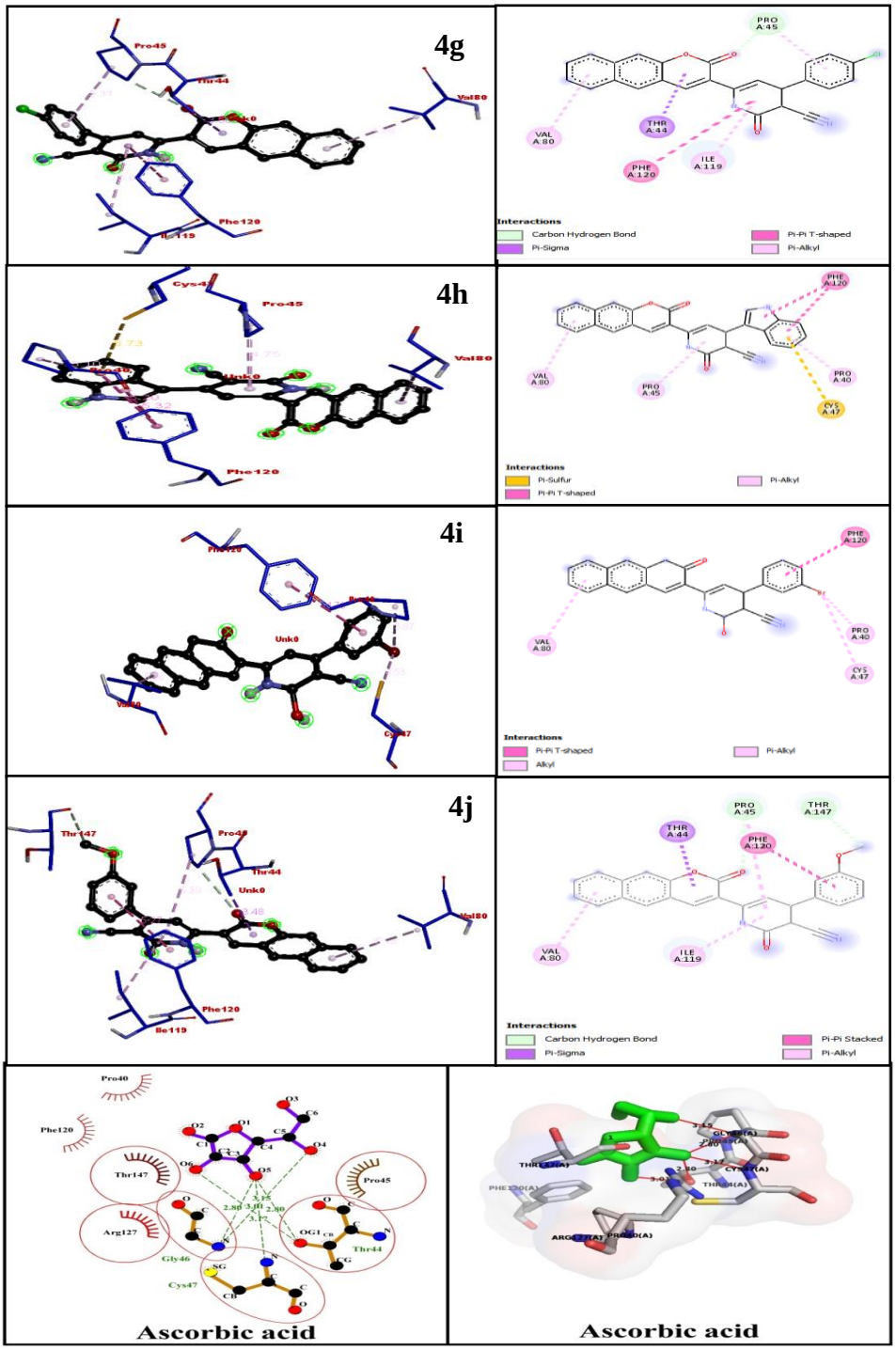

Figure 6 Three-dimensional and two-dimensional representations of molecular interactions between human peroxiredoxin 5 protein and synthesized compounds (**4g–j**) and reference drug Ascorbic acid.

Hence, there was no possibility of causing harmful toxicants to appear in the brain and blood stream. If the molecules have more negative logK_p value, it means that they possess lower skin permeation [44]. This is true for our synthesized compounds, which have more negative logK_p values in the range of –5.41 to –6.46 cm/s (Table S5).

Metabolism plays an important role in the bioavailability of drugs as well as drug-drug interactions [45]. Metabolism parameters are important to understanding whether the compounds act as a substrate or a non-substrate of the certain proteins. Hence, all the synthesized compounds were evaluated for the metabolism parameters, and the results showed that the compounds (**4a–j**) are non-substrates of permeability glycoprotein (P-gp), CYP1A2, CYP2C19, CYP2D6 and CYP3A4 inhibitors. The P-gp is an efflux membrane transporter, which is widely distributed throughout the body and is responsible for limiting cellular uptake and the distribution of xenobiotic and toxic substances [46]. The compounds (except for **4c** and **4e**) were found to be non-substrates of CYP1A2 inhibitors. Compounds **4b**, **4d**, **4f**, **4g** and **4i** were found to be substrates of CYP2C19 inhibitors, and the remaining compounds were non-substrates of CYP2C19 inhibitors.

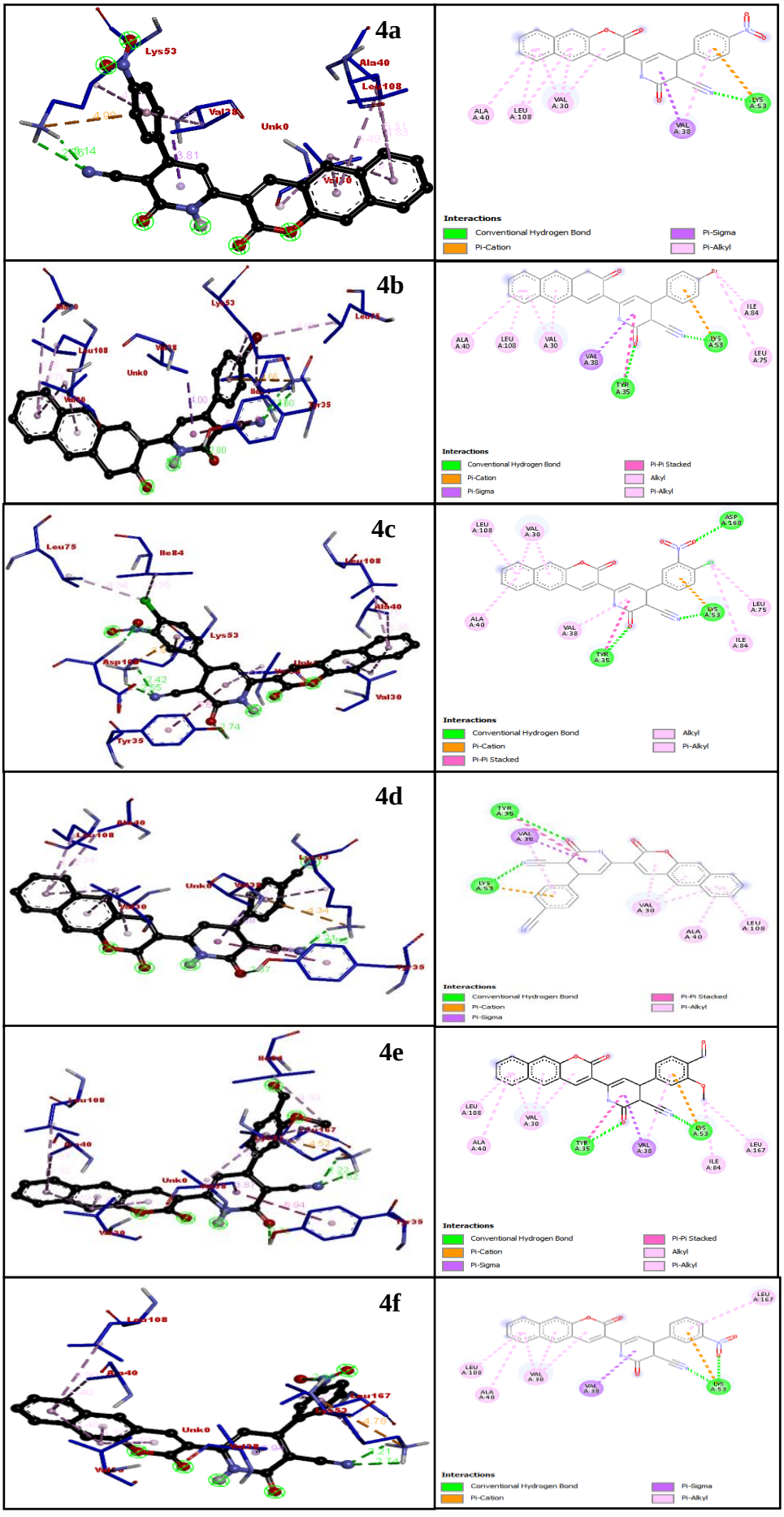

Figure 7 Three-dimensional and two-dimensional representations of molecular interactions between P38 MAP kinase protein and synthesized compounds (**4a–f**).

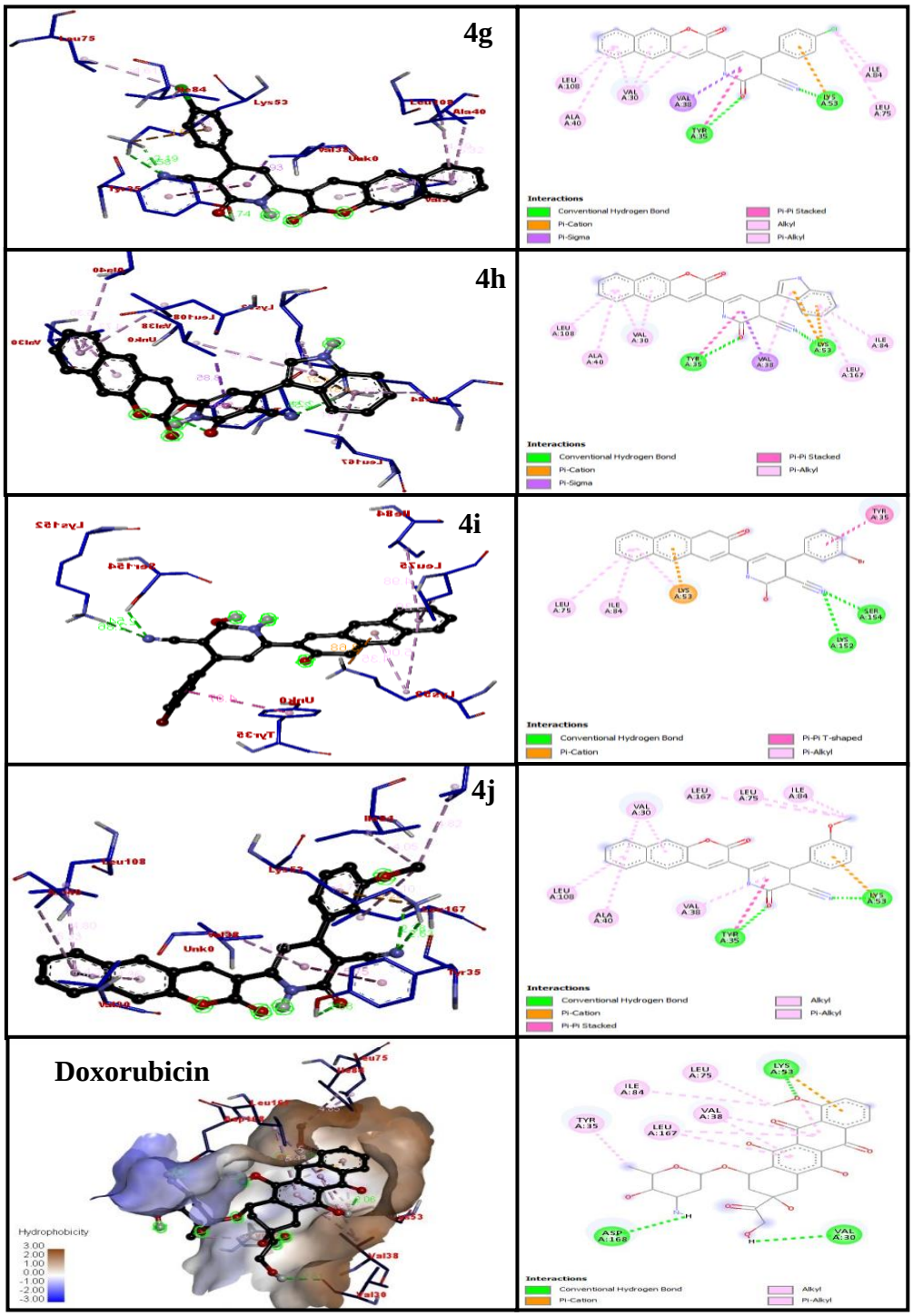

Figure 8 Three-dimensional and two-dimensional representations of molecular interactions between P38 MAP kinase protein and synthesized compounds (**4g–j**) and reference drug Doxorubicin.

All the compounds were found to be substrates of CYP2C9 inhibitors. The compounds (except for **4a, 4c, 4f, 4g, 4h**) are non-substrates to CYP2D6 inhibitors. All the compounds are non-substrates of CYP3A4 inhibitors. The data are listed in Table S6.

4. Conclusions

In this present work, we synthesized some novel 4-(substitutedphenyl)-1,2-dihydro-2-oxo-6-(2-oxo-2H-benzo[g]chromen-3-yl) pyridine-3-carbonitrile derivatives **4(a–j)** through the one-pot reaction. The antibacterial activity results show good efficacy against four bacterial strains. The antioxidant activity results suggested that compound **4d** exhibited the lowest IC_{50} value of 22.60±0.30. Compound **4b** displayed significant cytotoxic effect with an IC_{50} value of 34.66±2.43 as compared to the other compounds. The *in silico* docking studies suggested that the synthesized compounds interacted effectively with Human peroxiredoxin 5 and P38 MAP kinase proteins with good binding energy. In that, compounds **4h** and **4d** show the lowest binding energy values of –8.5 kcal/mol and –11.0 kcal/mol, respectively.

ADME studies explained that our synthesized compounds obeyed all the five rules with good bioavailability. Pharmacokinetic parameters suggested that the compounds have GI absorption, do not cross the blood-brain barrier, possess low skin permeation, and that there is no possibility of creating harmful toxicants. Based on the obtained results, the synthesized compounds are promising materials in the pharmacological fields.

Supplementary materials

Supplementary materials are available.

Funding

None.

Acknowledgments

The authors are grateful to the Chairman, Department of Chemistry, Kuvempu University, Shankaraghatta, for providing the laboratory facilities. One of the authors, MuthipeedikaNibin Joy is grateful to Russian Science Foundation (Grants No. 22-23-20189 and 21-13-00304). The authors are also grateful to SAIF, Karnataka University, Dharwad for providing the spectra and to Maratha Mandal, Belagavi for biological studies.

Author contributions

Conceptualization: M.G.V, Y.D.B.
Data curation: M.G.V, Y.D.B.
Formal Analysis: M.G.V, Y.D.B.
Investigation: M.G.V, Y.D.B.
Methodology: M.G.V, Y.D.B.
Project administration: Y.D.B., M.N.J.
Software: S.H.
Supervision: Y.D.B.
Validation: M.G.V., Y.D.B., M.N.J.
Visualization: M.G.V, Y.D.B.
Writing – original draft: M.G.V, Y.D.B.
Writing – review & editing: M.G.V, Y.D.B.

Conflict of interest

The authors declare no conflict of interest.

Additional information

Author IDs:
Yadav D. Bodke, Scopus ID 6504415850;
Muthipeedika Nibin Joy, Scopus ID 56072237200.

Websites:
Kuvempu University, http://www.kuvempu.ac.in/eng;
Jain University, https://www.jainuniversity.ac.in;
Ural Federal University, https://urfu.ru/en.

References

1. Kontogiorgis C, Anastasia D, Hadjipavlou-Litina D. Coumarin-based drugs: a patent review (2008-present). Expert Opin Ther Patents.2012;22:437–454. doi:10.1517/13543776.2012.678835
2. Narale VS. Synthesis of coumarin and their derivatives with their applications by different methods. World J Pharm Res. 2018;8:336–342. doi:10.20959/wjpr20188-11873
3. Bhattarai N, Kumbhar AA, Pokharel RY, Yadav PN. Anticancer potential of coumarin and its derivatives. Mini Rev Med Chem. 2021;21:2996–3029. doi:10.2174/1389557521666210405160323
4. Femy Maria KM, Sneha Antony, Amala Babu, Vinod B, Daisy PA. A meticulous review on coumarin derivatives as a marvel medication for thousands of ailments. Int J Pharm Sci Rev Res. 2021;30:242–253. doi:10.47583/ijpsrr.2021.v70i02.030
5. Borges F, Roleira F, Milhazes N, Santana L, Uriarte E. Simple coumarins and analogues in medicinal chemistry occurrence synthesis and biological activity. Curr Med Chem. 2005;12:887–916. doi:10.2174/0929867053507315
6. Luo KW, Sun JG, Chan JW, Yang L, Wu SH, Fung KP, Liu FY. Anticancer effects of imperatorin isolated from Angelica dahurica: induction of apoptosis in HepG2 cells through both death-receptor-and mitochondria mediated pathways. Chemother. 2011;57:449–459. doi:10.1159/000331641
7. Spino C, Dodier M, Sotheeswaran S. Anti-HIV coumarins from Calophyllum seed oil. Bioorg Med Chem Lett. 1998;8:3475–3478. doi:10.1016/S0960-894X(98)00628-3
8. Poole SK, Poole CF. Thin-layer chromatographic method for the determination of the principal polar aromatic flavour compounds of the cinnamons of commerce. 1994;119:113–120. doi:10.1039/an9941900113
9. Rosselli S, Maggio AM, Faraone N, Spadaro V, Morris-Natschke SL, Bastow KF, Lee HK, Bruno M. The cytotoxic properties of natural coumarins isolated from roots of Ferulago campestris (Apiaceae) and of synthetic ester derivatives of aegelinol. Nat Prod Commun. 2009;4:1701–1706.doi:10.1177/1934578X0900401219
10. Whang WK, Park HS, Ham I, Oh M, Namkoong H, Kim HK, Hwang DW, Hur SY, Kim TE, Park YG. Natural compounds. fraxin and chemicals structurally related to fraxin protect cells from oxidative stress. Exp Mol Med.2005;37:436–446. doi:10.1038/emm.2005.54
11. Crichton EG, Waterman PG. Dihydromammea c/ob: a new coumarin from the seed of Mammea Africana. Phytochem. 1978;17:1783–1786. doi:10.1016/S0031-9422(00)88695-1
12. Fort D, Rao K, Jolad S, Luo J, Carlson T, King S. Antihyperglycemic activity of Teramnus labialis (Fabaceae). Phytomed. 2000;6:465–467. doi:10.1016/S0944-7113(00)80075-6
13. Shin E, Choi KM, Yoo HS, Lee CK, Hwang BY, Lee MK. Inhibitory effects of coumarins from the stem barks of Fraxinus rhynchophylla on adipocyte differentiation in 3T3-L1 cells. Biol Pharm Bull. 2010;33:1610–1614.doi:10.1248/bpb.33.1610
14. Piller N. A comparison of the effectiveness of some anti-inflammatory drugs on thermal oedema. Br J Exp Pathol. 1975;56:554–559.
15. Jyoti D, Singla R, Kumar M, Vikas Jaitak. Recent developments of C-4 substituted coumarin derivatives as anticancer agents. Eur J Med Chem. 2016;119:141–168. doi:10.1016/j.ejmech.2016.03.087
16. Stanchev S, Momekov, Jensen G, Manolov FI. Synthesis, computational study and cytotoxic activity of new 4-hydroxycoumarin derivatives. Eur J Med Chem. 2008;43:694–706. doi:10.1016/j.ejmech.2007.05.005
17. Thornes RD, Daly L, Lynch G, Breslin B, Browne H, Corrigan HY, Daly P, Edwards G, Gaffney E. Treatment with coumarin to prevent or delay recurrence of malignant melanoma. Cancer Res Clin Oncol. 1994;120:32–34. doi:10.1007/BF01377122
18. Mohler JL, Gomella LG, Crawfrdo ED, Glode LM, Zippe Fair CD, Marshall WR. Phase II Evaluation of Coumarin (1,2-Benzopyrone) in metastatic prostatic carcinoma. Prostate. 1992;20:123–131. doi:10.1002/pros.2990200208

19. Rodney C, Richie MD, FACP, FCCP, John O, Swanson MD. Breast cancer: a review of the literature. J Insur Med. 2003;35:85–101.
20. Niinivehmas S, Pentikäinen OT. Coumarins as tool compounds to aid the discovery of selective function modulators of steroid hormone binding proteins. Mol. 2021;26:5142. doi:10.3390/molecules26175142
21. Song F, Huo X, Guo Z. Anti-breast cancer potential of natural and synthetic coumarin derivatives. Curr Top Med Chem. 2021;21:1692–1709. doi:10.2174/1568026621666210303145430
22. Braca A, De Tommasi N, Di Bari L, Pizza C, Politi M, Morelli I. Antioxidant principles from bauhinia tarapotensis. J Nat Prod. 2001;64:892–895. doi:10.1021/np0100845
23. Kenchappa R, Bodke YD, Telkar S, Nagaraja O. Synthesis and antimicrobial activity of fused isatin and diazepine derivatives derived from 2-acetyl benzofuran. Russ J Gen Chem.2017;87:2027–2038. doi:10.1134/S1070363217090195
24. Shridhar C, Ghagane, Sridevi I, Puranik, Vijay Kumbar M. *In vitro* antioxidant and anticancer activity of Leeaindica leaf extracts on human prostate cancer cell lines. Integr Med Res.2017;6:79–87. doi:10.1016/j.imr.2017.01.004
25. Joy MN, Bodke YD, Telkar S, Bakulev VA. Synthesis of coumarins linked with 1,2,3-triazoles under microwave irradiation and evaluation of their antimicrobial and antioxidant activity. J Mex Chem Soc. 2020;64:53–73. doi:10.29356/jmcs.v64i1.1116
26. Ghafar SZA, Mediani A, Maulidiani NSR, Abas F. Antioxidant, α-glucosidase and nitric oxide inhibitory activities of phyllanthusacidus and LC– MS/MS profile of the active extract. Food Biosci. 2018;18:1–28. doi:10.1016/j.fbio.2018.08.009
27. Joy MN, Bodke YD, Telkar S. 4-Methyl-7-alkynyl coumarin derivatives as potent antimicrobials and antioxidants. Bulg Chem Commun. 2020;52:237–244. doi:10.34049/bcc.5091
28. Kumbar VM, Peram MR, Kugaji MS, Shah T, Patil SP, Muddapur UM, Bhat KG. Effect of curcumin on growth, biofilm formation and virulence factor gene expression of porphyromonasgingivalis. Odontol. 2020;1:148–156. doi:10.1007/s10266-020-00514
29. Pandith A, Dasagrandhi C, Kim HR, Kim HS. Selective discrimination of putrescine and cadaverine based on a Fe^{3+}-morpholinoanthracene ensemble in solution and solid state and logic gate aided biological applications in mixed aqueous medium. Sens Actuators B Chem. 2017;1–37. doi:10.1016/j.snb.2017.07.115
30. Venkatesh T, Bodke YD, Aditya Rao SJ. Facile CAN catalyzed one pot synthesis of novel indol-5,8-pyrimido[4,5-d]pyrimidine derivatives and their pharmacological study. Chem. Data Collect. 2020;25;1–13. doi:10.1016/j.cdc.2019.100335
31. Hussein K, Eswaramoorthy R, Melaku Y, Endale M. Antibacterial and Antioxidant Activity of isoflavans from the Roots of Rhynchosiaferruginea and *in silico* study on DNA gyrase and human peroxiredoxin. Int J Second Metabol.2021;8:321–336. doi:10.21448/ijsm.962120
32. Aditya Rao SJ, Ramesh CK, Raghavendra S, Paramesha M. Dehydroabietylamine A diterpene from carthamustinctorious L. showing antibacterial and anthelmintic effects with computational evidence. Curr Comput Aided Drug Des. 2020;16:231–237. doi:10.2174/1573409915666190301142811
33. Swamy GK, Ramesh G, Pruthviraj K, Banu S, Roopa B, Preritha HJ, Rajeshwari BS, Ravikumar Shetty PR, Aruna Kumar DB, Sreenivasa S. *In silico* ADME, Molecular docking and cyclic voltammetry studies of 1, 4, 5-trisubstituted 1, 2, 3-triazole ethanone and ethanol derivatives via Metal free approach. Chem Data Collect. 2020;28:1–23. doi:10.1016/j.cdc.2020.100452
34. Lipinski CA, Lombardo F, Dominy BW, Feeney PJ. Experimental and computational approaches to estimate solubility and permeability in drug discovery and development settings. Adv Drug Deliv Rev. 1997;23:3–25. doi:10.1016/S0169-409X(96)00423-1
35. Raghavendra S, Aditya Rao SJ, Ramesh CK, Kumar. Multiple ligand simultaneous docking (MLSD): A novel approach to study the effect of inhibitors on substrate binding to PPO. Comput Biol Chem. 2015;59:81–86. doi:10.1016/j.compbiolchem.2015.09.008
36. Sander T, Freyss J, Von Korff M. Rufener Data Warrior C: An open-source program for chemistry aware data visualization and analysis. J Chem Inf Model. 2015;55:460–473. doi:10.1021/ci500588j
37. Joy MN, Bodke YD, Telkar S. 4-Methyl-7-Amino/Amido Coumarin derivatives as potential antimicrobials and antioxidants. Chem Nat Compd. 2020;56:614–620, doi:10.1007/s10600-020-03106-y
38. Haredi AA, Eldeeb MM, El-Naggar, Temairk H, Mohamed MA. Novel, quinazolin-2, 4-dione hybrid molecules as possible inhibitors against malaria: synthesis, and *in silico* molecular docking studies. Front Mol Biosci.2020;7:1–19. doi:10.3389/fmolb.2020.00105
39. Lipinski CA. Lead- and drug-like compounds: the rule-of-five revolution. Drug Discov Today Technol. 2004;1:337–341. doi:10.1016/j.ddtec.2004.11.007
40. Muegge I. Selection criteria for drug-like compound. Med Res Rev. 2003;23:302–321. doi:10.1002/med.10041
41. Breemen RB, Li van Y. Caco-2 cell permeability assays to measure drug absorption. Expert Opin Drug Metab Toxico. 2005;1:175–185. doi:10.1517/17425255.1.2.175
42. Alam S, Khan F. Virtual screening, docking, ADMET and system pharmacology studies on garcinia caged xanthone derivatives for anticancer activity. Sci Rep. 2018;8:1–16. doi:10.1038/s41598-018-23768-7
43. Rohitash Y, Mohammed I, Puneet D, Dheeraj KC, Shailendra H. Virtual screening, ADMET prediction and dynamics simulation of potential compounds targeting the main protease of SARS-CoV-2. J Biomol Struct Dyn.2021;39:6617–6632. doi:10.1080/07391102.2020.1796812
44. Mishra S, Dahima R. *In vitro* ADME studies of TUG-891, a GPR-120 inhibitor using SWISSADME predictor. J Drug Deliv Ther. 2019;9:366–369. doi:10.22270/jddt.v9i2-s.2710
45. Swamy GK, Ramesh G, Pruthviraj K, Salma Banu, Roopa B, Preritha HJ, Rajeshwari BS, Ravikumar M, Raghuram Shetty P, Aruna Kumar DB, Sreenivasa S. Synthesis, characterization, PASS prediction, *in silico* ADME, molecular docking and cyclic voltammetry studies of 1, 4, 5-trisubstituted 1, 2, 3-triazole ethanone and ethanol derivatives via metal free approach. Chem Data Collect.2020;28:1–23. doi:10.1016/j.cdc.2020.100452
46. Md. Lutful Amin. P-glycoprotein Inhibition for optimal drug delivery. Drug Target Insights. 2013:7:27–34. doi:10.4137%2FDTI.S12519